Detection and Localization of Unauthorized Unmanned Aerial Vehicle Operator using Unmanned Aerial Vehicle

Prusayon Nintanavongsa* and Itarun Pitimon*

Received : November 29, 2019
Revised : December 23, 2019
Accepted : December 25, 2019

Abstract

Unmanned Aerial Vehicle (UAV) has gained popularity recently, in both commercial and leisure purposes. Thanks to the technological advancement and dramatically lower manufacturing cost, UAV becomes very affordable and widely accessible to the public. This poses several critical security issues, ranging from merely loss of privacy to life-threatening incident. Consequently, it is crucial to be able to detect and locate an unauthorized UAV operator in case of critical security breach occurs. We propose a system to detect and locate an unauthorized UAV operator using UAV. This UAV, equipped with a directional antenna, performs unauthorized UAV operator detection and localization tasks by traveling along the predefined path and narrows down the potential area as time passes. The key performance metrics under investigation are coverage area, identifiable area, time to identify an unauthorized UAV operator, and error rate. We demonstrate, through simulation studies, how UAV service ceiling, UAV speed, and antenna directivity have an effect on the key performance metrics of the system, together with, the optimal operating condition.

Keywords: Unmanned Aerial Vehicle, Detection, Localization, Unauthorized Operator.

1. Introduction

UAV is one of the emerging technologies that has seen a major growth in the recent years. It has secured its places in several applications, ranging from civil to military uses. Civil use of UAV includes aerial photography, filmmaking, and agricultural monitoring while aerial surveillance and reconnaissance are examples of UAV applications for military use. One of the key features that makes UAV attractive is the ability to provide the aerial perspective and its freedom of movement without the need of infrastructure, i.e., roads and electrical facilities. Consequently, it is undeniable that UAV will soon become the workhorse in aerial related applications. In fact, it already replaces human-operated aircraft in aerial photography business since it not only provides a significantly lower in operating cost but also eliminates the human risk involved in operating an actual aircraft. It is globally estimated the market worth of $4.1 billion in commercial UAVs in 2017 and it is expected over 7 million UAVs registration in the United States by 2020 [1].

Since UAV is easily accessible and affordable, several issues involving illegal uses of UAV are increasing rapidly. Breaching of privacy through unauthorized UAV operation is commonly found in most cases. The charge of unauthorized UAV operation spans from misdemeanor to felony offense, depending on the territory the offense occurs [ncsl.org]. However, in an extreme case, i.e., using UAV for malicious purposes, it is not only required that the hostile UAV be rendered harmless but also the need to identify the operator of the hostile UAV. Rendering UAV harmless can be achieved through the use of UAV jammer. UAV jammer interferes the communication between UAV and its operator. As a result, the targeted UAV either drops to the ground or returns to its initial location. Note that the UAV operator is fully aware of the jamming and mostly flees from the scene. Hence, the UAV jammer can prevent malicious UAV from accomplishing its

* *Department of computer engineering, Faculty of engineering, Rajamangala University of Technology Thanyaburi.*

task but cannot locate and apprehend the hostile UAV operator.

There exist several methods to detect and locate an unauthorized signal source emitter, i.e., unauthorized UAV operator. Mobile signal tracker and existing communication infrastructures are good examples. However, these facilities are ground-based and have limitations in terms of difficulties in equipment deploying as well as the speed of detection and localization the unauthorized transmitting signal source. In fact, it is almost impossible to employ the existing communication infrastructures for unauthorized UAV detection and localization since they are designed for different purposes from the beginning.

Figure 1. *Detection and locaization with UAV at high service ceiling.*

Figure 1 shows our proposed system for detection and localization of an unauthorized UAV operator using UAV. Initially, the UAV starts of at a higher service ceiling in order to cover a large searching area. However, the location of an unauthorized UAV operator cannot be pinpointed but rather a rough estimate. To narrow down the potential area that an unauthorized UAV operator resides, the UAV identify the potential sector through received signal strength measurement and moves toward the potential sector. The UAV then lower the service ceiling in order to locate an unauthorized UAV operator in fine-grained manner as depicted in Figure 2. Note that the circle signifies the detection range of the UAV.

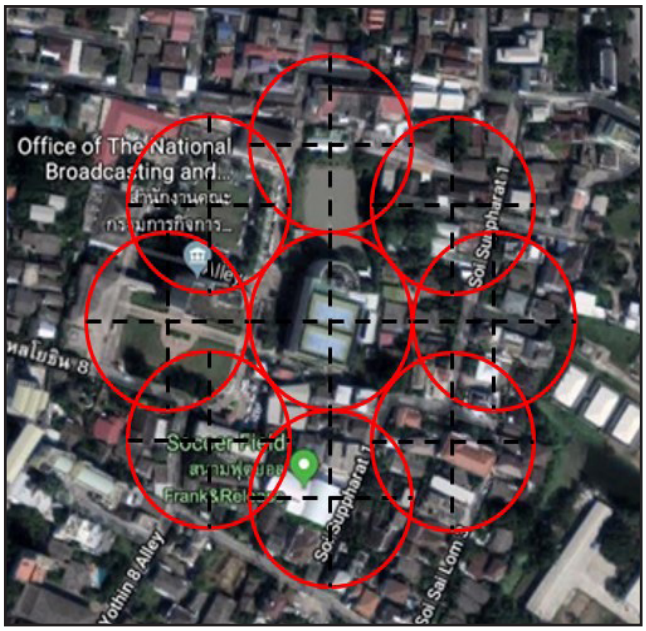

Figure 2. *Detection and locaization with UAV at low service ceiling.*

The major contributions of our work can be summarized as follows:

• We propose a system to detect and locate an unauthorized UAV operator using UAV. This UAV, equipped with a directional antenna, performs unauthorized UAV operator detection and localization tasks by traveling along the predefined path and narrows down the potential area as time passes.

• We demonstrate, through simulation studies, how UAV service ceiling, UAV speed, and antenna directivity have an effect on the key performance metrics of the system, together with, the optimal operating condition.

The rest of this paper is organized as follows: The related work is given in Section 2. The proposed system are discussed in details in Section 3. The simulation results are revealed in Section 4. Finally, Section 5 concludes our work.

2. Related Work

Detection and localization of an unauthorized signal source is not new but has been a topic of discussion for a long time. Several techniques have been proposed and received substantial attention from research community. Angle of Arrival (AoA) is a technique that determines the location of signal source by angle estimation between the direction of an incident wave

and a certain reference direction [2], [3], [4]. However, the drawback of AoA is that it is severely affected by non line-of-sight condition. Moreover, the accuracy of AoA is limited by the directivity of the antenna and channel fading, and multipath reflection. The concept of Time of Arrival (TOA) is discussed in [5], [6], [7]. In ToA method, the propagation time between the transmitter and the receiver is estimated by calculating the time difference between them, that is, transmitter's time and receiver's time. In [8], [9], [10], Time Difference of Arrival (TDoA), the localization method based on the measurement of the difference in the arrival times of the signal from the source at multiple nodes, is revisited. The advantage of TDoA is that it is marginally susceptible to multipath reflection and non line-of-sight condition. Lastly, the Received Signal Strength Indication (RSSI) is present in [11]-[15]. In this method, the strength of the received signal at the receiver is translated to the distance between the transmitter and the receiver using Friis transmission equation [16]. However, RSSI is susceptible to multipath reflection and channel fading. A multiplication distance correction factor is introduced in [17] to counteract estimation error and hence drastically improve the accuracy.

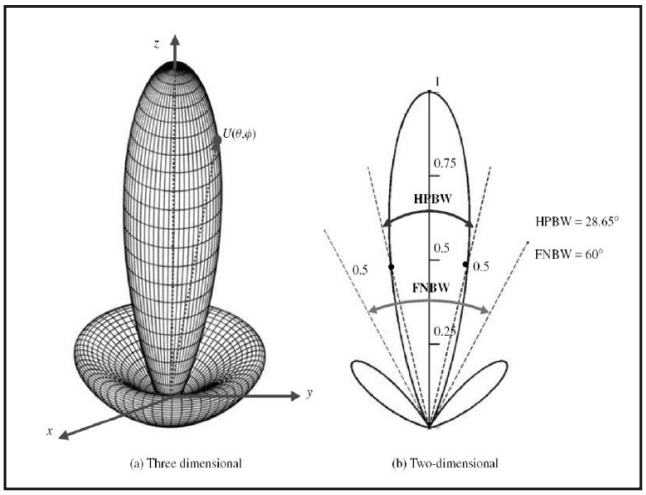

Figure 3. *Radiation pattern of the directional antenna.*

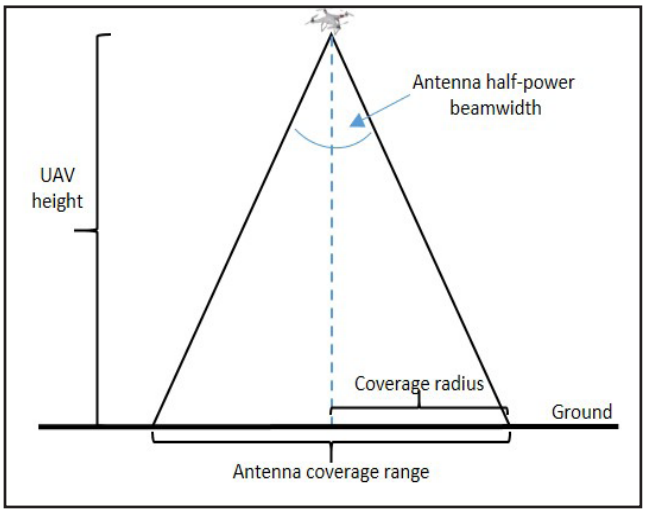

Figure 4. *Coverage area of the UAV equipped with directional antenna.*

3. The Proposed System

One of the key elements of the proposed system that enables an unauthorized UAV operator detection and localization is the directional antenna. The directional antenna is a good candidate for directional finding as it provides a high gain and hence a high sensitivity. However, the sensitivity of the directional antenna can be different according to the design. For example, the directional antenna with narrower beamwidth offers the higher sensitivity compared to the directional antenna with wider beamwidth. On the other hand, the directional antenna with wider beamwidth provides the larger coverage area compared to the directional antenna with narrower beamwidth.

The radiation and reception patterns of the directional antennas are characterized by their beamwidth. The Half Power Beamwidth (HPBW) is the angular separation in which the magnitude of the radiation pattern decreases by 3 dB from the peak of the main beam. Figure 3 illustrates the radiation pattern of the directional antenna and its HPBW. It is obvious that the larger the HPBW, the larger the coverage area of signal detection. Consequently, if the directional antenna is installed on the UAV in such the way that the directional antenna's main lobe is perpendicular to the ground, that is, the UAV is equipped with the directional antenna underneath and pointing downwards. The coverage area of this directional antenna equipped UAV is shown in Figure 4. The relationship between UAV service ceiling (UAV height), coverage radius, and HPBW is shown in Equation 1.

$$coverage\ radius = \tan\frac{HPBW}{2} \times uav\ height \quad (1)$$

It is shown in Equation 1. that the coverage radius is directly proportion to UAV height and HPBW. In other words, the coverage radius can be increased by increasing UAV height and HPBW. The coverage area, the area that the UAV can detect the presence of an unauthorized UAV operator, can be derived in Equation 2.

$$coverage\ area = \pi \times coverage\ radius^2 \quad (2)$$

3.1 Detection of an Unauthorized UAV Operator

The coverage area shown in Equation 2. is the area that the UAV can detect the presence of an unauthorized UAV operator. In order to provide larger coverage area, the UAV performs the flying pattern as depicted in Figure 5. The UAV begins detection of an unauthorized UAV operator at the sector A. Again, the circle signifies the detection range of the UAV, that is, the UAV is able to detect the presence of an unauthorized UAV operator if and only if it resides within the circle. Once it accomplishes detection of an unauthorized UAV operator at the sector A, it then proceeds to the sector B and performs detection of an unauthorized UAV operator. Upon completing the detection of an unauthorized UAV operator in sector B, it moves towards the sector C and performs detection of an unauthorized UAV operator. The process carries on in this fashion, a clockwise progression, until it finally reaches the destined sector I. Upon finishing the round of detection, the coverage area of that round can be calculated in Equation 3.

$$coverage\ area around_{round} = \pi \times (3 \times coverage\ radius)^2 \quad (3)$$

The signal power perceived by the UAV signifies the distance between the sensing UAV and an unauthorized UAV operator. In other word, the stronger the signal received by the sensing UAV, the closer the UAV to an unauthorized UAV operator. The Friis transmission equation describe the relationship of received power ($P_{receiver}$), transmitted power ($P_{transmitter}$), and distance (d) between transmitter and receiver as shown in Equation 4.

$$p_{receiver} = p_{tranmitter} G_t G_r \left(\frac{c}{4\pi fd}\right)^2 \quad (4)$$

where G_t is the antenna gain of transmitter, G_r is the antenna gain of receiver, and are antenna gains, and $\left(\frac{c}{f}\right)$ is the wavelength of the transmitted signal. It is clear that the received signal strength, diminishes with the square of the distance.

As mentioned previously, the circle in Figure 5 signifies the detection range of the UAV. This implies that the maximum degree of separation, that enables the detection of an unauthorized UAV operator, between the sensing UAV and an unauthorized UAV operator lies on the perimeter of the circle. This the maximum degree of separation is simply the hypotenuse in Figure 4. Consequently, it can be calculated as in Equation 5.

$$distance_{max} = \frac{uav\ height}{\cos\left(\frac{HPBW}{2}\right)} \quad (5)$$

The lowest level of received signal that the UAV can detect the presence of an unauthorized UAV operator is then derived in Equation 6

$$p_{receiver\_\min} = p_{tranmitter} G_t G_r \left(\frac{c}{4\pi f\ distance_{\max}}\right)^2 \quad (6)$$

The signal power received by the UAV in each sector is recorded and will be used in the next section, Localization of an unauthorized UAV operator.

3.2 Localization of an Unauthorized UAV Operator

After completion of the detection of an unauthorized UAV operator in each sector, the next phase is to determine the potential sector that an unauthorized UAV operator most likely resides. The signal power received by the UAV in each sector are compared. As mentioned earlier, the stronger the signal received by the sensing UAV, the closer the UAV to an unauthorized UAV operator. Hence, the potential sector that an unauthorized UAV operator most likely resides is the sector that has the highest level of received signal.

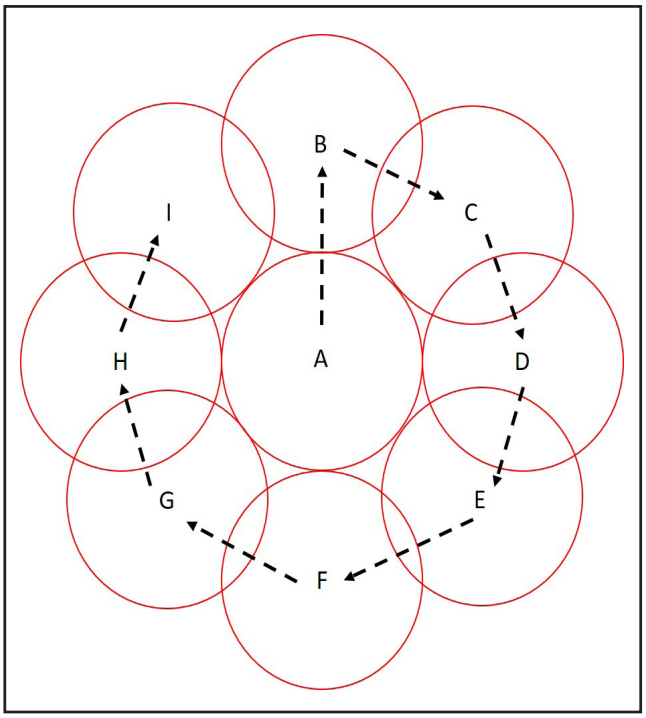

Figure 5. *UAV flying pattern for detection and localization of an unauthorized UAV operator.*

Given that the coverage radius of the UAV is r, and the centroid of sector A is located at coordinate(X_A, Y_A, Z_A), the centroid of each sector depicted in Figure 5. can be found as follows:

$$\textit{Centroid A}: (X_A, Y_A, Z_A) \quad (7)$$

$$\textit{Centroid B}: (X_B, Y_B, Z_B) = (X_A, Y_A+2r, Z_A) \quad (8)$$

$$\textit{Centroid C}: (X_C, Y_C, Z_C) = (X_A+\sqrt{2r}, Y_A+\sqrt{2r}, Z_A) \quad (9)$$

$$\textit{Centroid D}: (X_D, Y_D, Z_D) = (X_A+2r, Y_A, Z_A) \quad (10)$$

$$\textit{Centroid E}: (X_E, Y_E, Z_E) = (X_A+\sqrt{2r}, Y_A-\sqrt{2r}, Z_A) \quad (11)$$

$$\textit{Centroid F}: (X_F, Y_F, Z_F) = (X_A, Y_A+2r, Z_A) \quad (12)$$

$$\textit{Centroid G}: (X_G, Y_G, Z_G) = (X_A-\sqrt{2r}, Y_A-\sqrt{2r}, Z_A) \quad (13)$$

$$\textit{Centroid H}: (X_H, Y_H, Z_H) = (\mathrm{X}_A\text{-}2\mathrm{r}, \mathrm{Y}_A, \mathrm{Z}_A) \quad (14)$$

$$\textit{Centroid I}: (X_I, Y_I, Z_I) = (X_A-\sqrt{2r}, Y_A+\sqrt{2r}, Z_A) \quad (15)$$

Once the sector with the highest level of received signal is determined, it is the most likely that an unauthorized UAV operator lies within the sector. The centroid of that corresponding sector is used as the initial sector for the detection of an unauthorized UAV operator in the next round. In other words, the centroid of that corresponding sector becomes the centroid of sector A in the next round of detection of an unauthorized UAV operator.

3.3 UAV Repositioning

Once the potential sector is determined in the previous section, the UAV needs to proceed to the new coordinate and perform the next round of detection of an unauthorized UAV operator. However, only relocating the centroid in X and Y axis will not contribute to the better resolution in detection and localization of an unauthorized UAV operator. It is imperative that the service ceiling of the UAV be lowered in order to capture the signal with higher resolution and hence the more precise localization of an unauthorized UAV operator. We introduce the UAV descending scale, defined as the scaling factor that UAV exhibits in lowering its service ceiling. For example, if the service ceiling of the UAV is at 1000 meters in the first detection round, with the UAV descending scale of 2, the next service ceiling of the UAV in the next round will be 500 meters. UAV descending scale has to be chosen carefully, too large UAV descending scale can lower time to identify the location of an unauthorized UAV operator while too small UAV descending scale can significantly increase time to identify the location of an unauthorized UAV operator and render the system unresponsive. Nevertheless, there is a flip side to the coin. , too large UAV descending scale can result in higher error detection rate of an unauthorized UAV operator while small UAV descending scale can drastically improve detection accuracy of the system.

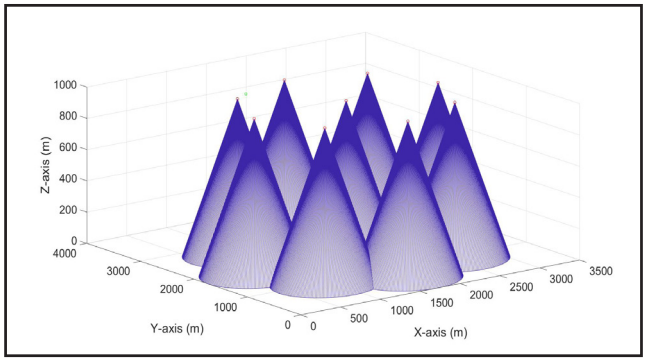

Figure 6. *Coverage area of the proposed system at UAV service ceiling of 1000 meters.*

3.4 System Operation Example

In order to better understand how the system progresses through different stages of detection and localization of an unauthorized UAV operator. We illustrates the system progression starting at the UAV service ceiling of 1000 meters. Figure 6 shows the coverage area of the proposed system at UAV service ceiling of 1000 meters. The coverage area of each sector is represented by the cone for each corresponding sector. Consequently, there are 9 cones which correspond to 9 sectors, that is, sector A to sector I. Moreover, the peak of each cone refers to the location that the UAV hovers while performing detection of an unauthorized UAV operator. The UAV starts at sector A then proceeds to sector B, sector C, and so on. Finally, it completes the round of detection of an unauthorized UAV operator at sector I.

Another perspective of the coverage area of the proposed system at UAV service ceiling of 1000 meters can be seen in Figure 7. Here, the top view of the coverage area of each sector, together with the location of an unauthorized UAV operator in sector I, is presented. It is obvious that each sector has its own coverage and contributes to the larger coverage as a whole.

The two dimensional representation of the coverage area of the proposed system can also be depicted in Figure 8. Here, the side view of the coverage area of the proposed system at UAV service ceiling of 1000 meters is shown and it provides a clear represention of the coverage beam of each sector.

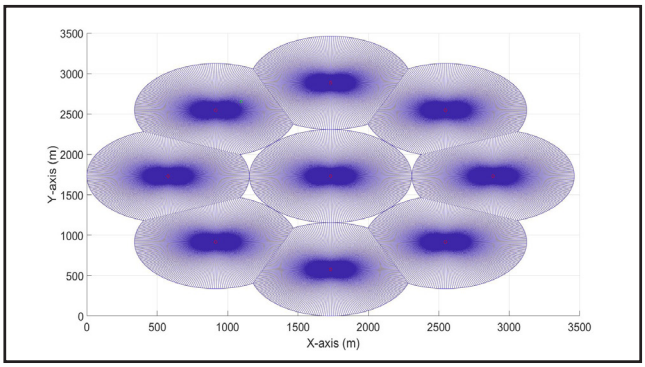

Figure 7. *Coverage area of the proposed system at UAV service ceiling of 1000 meters (top view).*

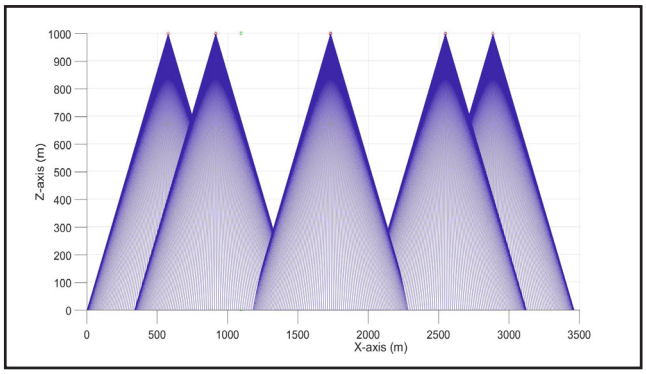

Figure 8. *Coverage area of the proposed system at UAV service ceiling of 1000 meters (side view).*

Once the UAV completes the round of detection, the system performs the localization by selecting the potential sector to be the centroid of the next detection round. In this case, since the location of an unauthorized UAV operator is in sector I, the received signal power of sector I is the highest among all sectors. Hence, the centroid of sector I is chosen to be centroid of sector A in the next detection round. The localization process is completed at this point.

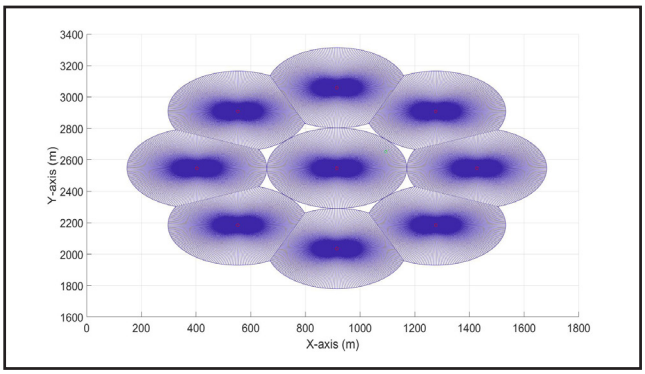

Figure 9. *Coverage area of the proposed system at UAV service ceiling of 444 meters (top view).*

The next stage of the system is to reposition the UAV, that is, lowering its service ceiling to better capture the signal resolution. In Figure 9, the UAV descending scale used is 2.25 and the new UAV service ceiling is 444 meters. The centroid of sector I in the previous detection round becomes the centroid of sector A for the present detection round. The UAV then reiterates through sector A to sector I, like the previous detection round, and records its findings in each sector for localization process.

The system proceeds through rounds of detection repetitively and finally halts when the predefined UAV service ceiling is achieved, 39 meters in this case. The final round of detection and localization of an unauthorized UAV operator terminates at this point and the corresponding top view of the proposed system can be seen in Figure 10.

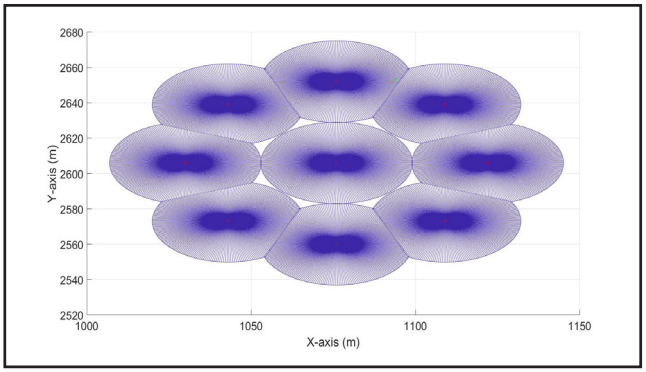

Figure 10. *Coverage area of the proposed system at UAV service ceiling of 39 meters (top view).*

4. Simulation Results

In this section, we thoroughly evaluate our proposed system using our custom simulator, developed in MATLAB. We investigate the effect of UAV service ceiling, UAV speed, and antenna directivity on the key performance metrics of the system. Unless specifically stated, the simulation time is limited to 1,500 seconds and an unauthorized UAV operator is deployed uniformly at random in 2,500 m2 circular area. The number of iterations for each complete process of detection and localization of an unauthorized UAV operator is set to 50 and the result is obtained through the average value of 50 iterations. This is to prevent outliers from influencing the simulation results.

4.1 Coverage Area

The coverage area is one of key performance metrics since it has a major effect on system efficiency, that is, system efficiency is directly proportion to the coverage area. In other words, the larger the coverage area, the faster the detection and localization of an unauthorized UAV operator and hence the higher the system efficiency. Figure 11 depicts the effect of UAV height on coverage area of the proposed system for various values of HPBW. It is clear that, for the HPBW value of 60 and 90 degrees, the coverage area exhibits a nonlinear increase with increasing UAV height. Consequently, it is preferable to initiate the UAV service ceiling at higher altitude in order to cover a larger area. On the other hand, the UAV equipped with antenna with HPBW of 60 degrees sees negligible benefit on this matter.

The benefit of the proposed system is clearly see in Figure 11. For example, if we initiate the UAV service ceiling at 1,000 meters with HPBW of 60 degrees, the coverage area of the system can be as large as 9 km2. In addition to large coverage area provided by the proposed system, it also offers a fine-grained localization of an unauthorized UAV operator. Figure 12 illustrates the fine-grained localization of an unauthorized UAV operator offered by the proposed system. It is obvious that the proposed system provides an almost pinpoint location of an unauthorized UAV operator. For instance, if the UAV service ceiling is lowered to 60 meters with HPBW of 60 degrees, the identifiable area of an unauthorized UAV operator can be as small as 400 m2.

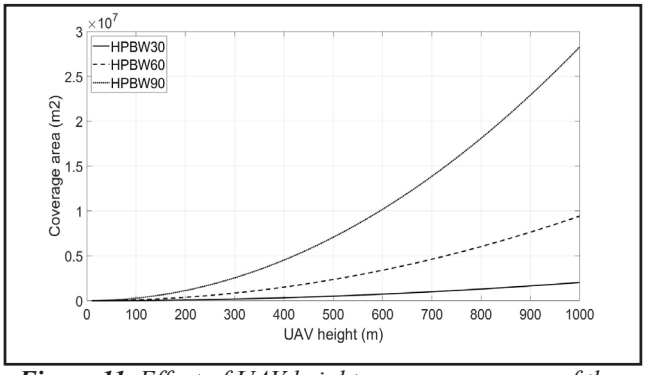

Figure 11. *Effect of UAV height on coverage area of the proposed system for various values of HPBW.*

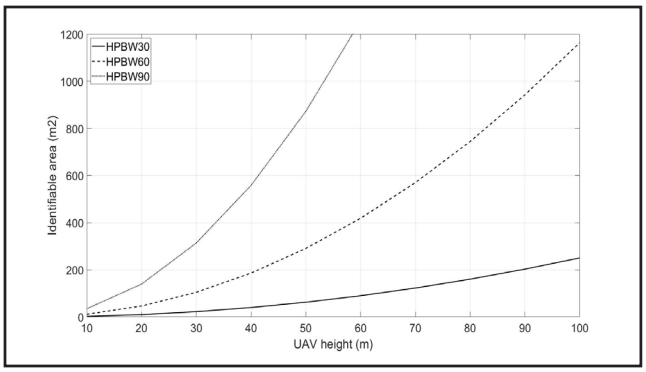

Figure 12. *Fine-grained localization of an unauthorized UAV operator.*

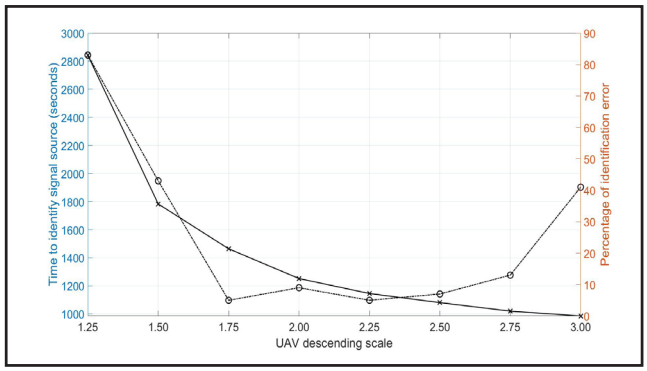

Figure 13. *Effect of UAV descending scale on time to identify an unauthorized UAV operator and its corresponding percentage of identification error.*

4.2 Time to Identify an Unauthorized UAV Operator

Time to identify an unauthorized UAV operator is defined as the time the system takes, from deploying the UAV until the location of an unauthorized UAV operator is determined. It is undeniable that this is the most important key performance metric of the system and it is also preferable to have the lowest value possible. The system that offers low time to identify signal source implies that the location of an unauthorized UAV can be determined promptly and further security measures can be carried out in timely manner. Moreover, since the UAV spends less time in the air, the energy consumption per detection and localization cycle is lower. As a result, the duty cycle of the system is higher and hence improving the system availability. Figure 13 depicts an effect of UAV descending scale on time to identify an unauthorized UAV operator and its corresponding percentage of identification error. As mentioned previously, UAV descending scale has to be carefully chosen as it can drastically affect the system performance. It is obvious that choosing an arbitrary value of UAV descending scale is not a good idea. In this case, the UAV with HPBW of 60 degrees begins the detection of an unauthorized UAV operator at service ceiling of 1,000 meters. The UAV descending scale is varied from 1.25 to 3.00 with 0.25 step size. It is clear the time to identify an unauthorized UAV operator is not linearly dependent with the UAV descending scale, that is, the time to identify an unauthorized UAV operator exponentially increases once the UAV descending scale is less than 2.0 while it exhibits linear increase with decreasing value of UAV descending scale elsewhere.

It is straight forward to choose the largest value of UAV descending scale if the identification error is omitted. However, it is crucial to investigate as many aspects of the system. Here, the percentage of identification error, defined as the percentage that the system fails to determine the location of an unauthorized UAV operator, is examined for different values of UAV descending scale. It is interesting that it does not exhibits either linear or exponential behavior with UAV descending scale. On the contrary, the percentage of identification error decreases with decreasing value of UAV descending scale, remains constant shortly, and then increases with decreasing value of UAV descending scale. In other words, the percentage of identification error yields a local minima. Figure 13 provides an invaluable information about the optimal choice of UAV descending scale, that is, the value of UAV descending scale in which the system yields the optimal performance. It is obvious that the UAV descending scale of 2.35 is the optimal choice since it is where the time to identify signal source and percentage of identification error cross.

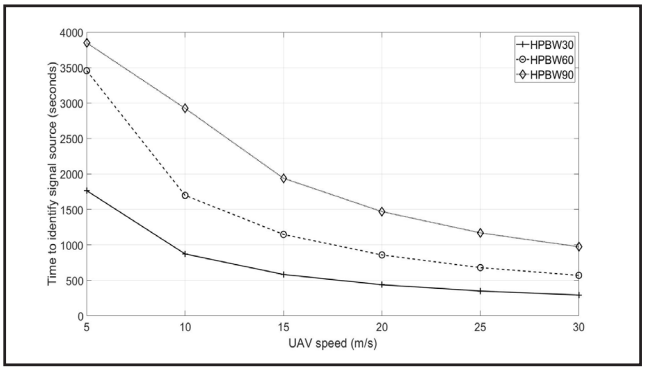

Figure 14. *Effect of UAV speed on time to identify an unauthorized UAV operator.*

The effect of UAV speed on time to identify an unauthorized UAV operator is shown in Figure 14. The UAV speed is varied from 1.25 to 3.00 with 0.25 step size and shown on X-axis while Y-axis shows the time to identify an unauthorized UAV operator. The system is set to terminate detection and localization when UAV service ceiling reaches 40 meters

which corresponds to 200 m2 of an identifiable area for UAV equipped with HPBE of 60 degrees. It is obvious that by increasing the UAV speed, the time to identify an unauthorized UAV operator decreases. Otherwise speaking, the time to identify an unauthorized UAV operator is inversely proportion to the UAV speed. However, the relationship among the two are not linear. The rate of reduction of the time to identify an unauthorized UAV operator is higher during UAV speed of 5 to 15 m/s while it tapers off towards higher UAV speed.

The HPBW of the antenna also has an effect on the time to identify an unauthorized UAV operator. Three values of HPBW, 30, 60, and 90 degrees, are investigated in Figure 14. It is clear that all value of HPBW exhibits a similar pattern and the antenna with smaller value of HPBW yields lower value of time to identify an unauthorized UAV operator. However, it should not be concluded that the antenna with a small value of HPBW is preferable since it also offers less coverage area compared to ones with a higher value of HPBW, and vice versa.

5. Conclusions

UAV has seen an exceptional growth in the recent past and it is highly affordable and accessible than ever before. This poses several critical security issues, ranging from merely loss of privacy to life-threatening incident. It is crucial for the system to not only intercept an unauthorized UAV but also able to locate an unauthorized UAV operator. We propose a system to detect and locate an unauthorized UAV operator by equipping the UAV with a directional antenna. This UAV performs an unauthorized UAV operator detection and localization tasks by traveling along the predefined path and narrows down the potential area as time passes. We demonstrate, through simulation studies, how UAV service ceiling, UAV speed, and antenna directivity have an effect on the key performance metrics of the system, together with, the optimal operating condition.

6. References

[1] Cooperative Surveillance for UAVs: Enabling safe, secured and efficient UAV operations, [Online] https://www.eurocontrol.int/sites/default/files/events/presentation/session5.5-thales-utm-aperspective.pdf

[2] R. Peng and M. L. S ichitiu, "Angle of arrival localization for wireless sensor networks." *In Proceedings of 3rd Annual IEEE Communications Society on Sensor and Adhoc Communications and Networks*, January, 2006.

[3] S. Tomic, M. Beko, and M. Tuba. "A linear estimator for network localization using integrated RSS and AOA measurements." *IEEE Signal Processing Letter*, Vol. 26, No. 3, pp. 405-409, March, 2019.

[4] N. Garcia, H. Wymeersch, and D. T. M. Slock. "Optimal precoders for tracking the AoD and AoA of a mmWave path." *IEEE Transactions on Signal Processing*, Vol. 66, No. 21, pp. 5718-5729, November 2018.

[5] C.-H. Park and J.-H. Chang. "TOA source localization and DOA estimation algorithms using prior distribution for calibrated source." *Digital Signal Processing,* Vol. 71, pp. 61-68, December, 2017.

[6] M. R. Gholami, S. Gezici, and E. G. Ström. "TW-TOA based positioning in the presence of clock imperfections." *Digital Signal Processing*, Vol. 59, pp. 19-30, December, 2016.

[7] Y. Liu, F. Guo, L. Yang, and W. Jiang. "Source localization using a moving receiver and noisy TOA measurements." *Signal Processing*, Vol. 119, pp. 185-189, February, 2016.

[8] E. Kazikli and S. Gezici. "Hybrid TDOA/RSS based localization for visible light systems." *Digital Signal Processing*, Vol. 86, pp. 19-28, March, 2019.

[9] D. Wang, J. Yin, T. Tang, X. Chen, and Z. Wu. "Quadratic constrained weighted least-squares method for TDOA source localization in the presence of clock synchronization bias: Analysis and solution." *Digital Signal Processing*, Vol. 82, pp. 237-257, November, 2018.

[10] Y. Sun, K. C. Ho, and Q. Wan. "Solution and analysis of TDOA localization of a near or distant source in closed form." *IEEE Transactions on Signal Processing*, Vol. 67, No. 2, pp. 320-335, January, 2019.

[11] P. Abouzar, D. G. Michelson, and M. Hamdi. "RSSI-based distributed self-localization for wireless sensor networks used in precision agriculture." *IEEE Transactions on Wireless Communications*, Vol. 15, No. 10, pp. 6638-6650, October, 2016.

[12] A. E. Lagias, T. D. Lagkas, and J. Zhang. "New RSSI-based tracking for following mobile targets using the law of cosines." *IEEE Wireless Communication Letter*, Vol. 7, No. 3, pp. 392-395, Junuary, 2018.

[13] J. Luomala and I. Hakala, "Analysis and evaluation of adaptive RSSI based ranging in outdoor wireless sensor networks." Ad Hoc Networks, Vol. 87, pp. 100-112, May, 2019.

[14] Z. Na, Y. Wang, X. Li, J. Xia, X. Liu, M. Xiong, and W. Lu. "Subcarrier allocation based simultaneous wireless information and power transfer algorithm in 5G cooperative OFDM communication systems." *Physics Communications*, Vol. 29, pp. 164-170, August, 2018.

[15] Z. Na, J. Lv, M. Zhang, B. Peng, M. Xiong, and M. Guan, "GFDM based wireless powered communication for cooperative relay system." *IEEE Access*, Vol. 7, pp. 50971-50979, April, 2019.

[16] T. S. Rappaport. *Wireless communications*, *principles and practice*. Prentice Hall, 1996.

[17] L. Gui, M. Yang, P. Fang, and S. Yang. "RSS-based indoor localization using MDCF." *IET Wireless Sensor Systems*, Vol. 7, No. 4, pp. 98-104, August 2017.